

Article

Effects of Calcium on the Removal of Ammonium from Aged Landfill Leachate by Struvite Precipitation

Hussein Rayshouni and Mahmoud Wazne *

Civil Engineering, Lebanese American University, 301 Bassil Building, Byblos P.O. Box 36, Lebanon;
hussein.rayshouni@lau.edu.lb

* Correspondence: mahmoud.wazne@lau.edu.lb

Abstract: Ammonium in landfill leachates is a major contributor to environmental degradation if not effectively treated. However, it could be converted to a valuable fertilizer when it is co-precipitated with phosphate and magnesium as struvite. Low-cost magnesium and phosphate sources are sought to offset the co-precipitation treatment costs, but most of the identified alternative magnesium sources have significant amounts of calcium, which may negatively impact the ammonium removal rates. In this study, the effects of calcium on ammonium removal from high-strength aged field landfill leachate as struvite were investigated. Laboratory-scale batch tests were conducted to assess the effects of the pH, $Mg^{2+}:NH_4^+:PO_4^{3-}$, and $Ca^{2+}:Mg^{2+}$ molar ratios on ammonium removal. Magnesium chloride salt was used as a model dissolved magnesium source, whereas different compounds derived from dolomite ($CaMg(CO_3)_2$) were used as model solid-phase magnesium sources. X-ray powder diffraction and activity ratio diagrams were used to delineate the ammonium removal mechanisms and struvite stability. The ammonium removal rate of the magnesium salt decreased from approximately 97% to 70%, upon increasing the $Ca^{2+}:Mg^{2+}$ molar ratio from 0 to 1.0, for the $Mg^{2+}:NH_4^+:PO_4^{3-}$ molar ratio of 1.25:1:1.25 and pH = 9.5. For similar pH values, as well as the $Mg^{2+}:NH_4^+:PO_4^{3-}$ and $Ca^{2+}:Mg^{2+}$ molar ratios, the ammonium removal rates by the dolomite-derived compounds reached up to 55%, which highlighted the limited availability of magnesium in solid phases, in addition to the negative impacts of calcium. The diffractometric analysis and thermodynamic calculations revealed the stable regions of struvite in the presence of competing solid phases. The new findings in this study could aid in the design of ammonium and phosphate removal and recovery systems by struvite precipitation.



Citation: Rayshouni, H.; Wazne, M. Effects of Calcium on the Removal of Ammonium from Aged Landfill Leachate by Struvite Precipitation. *Water* **2022**, *14*, 1933. <https://doi.org/10.3390/w14121933>

Academic Editors: Dibyendu Sarkar, Rupali Datta, Prafulla Kumar Sahoo and Mohammad Mahmudur Rahman

Received: 20 April 2022

Accepted: 21 May 2022

Published: 16 June 2022

Publisher's Note: MDPI stays neutral with regard to jurisdictional claims in published maps and institutional affiliations.



Copyright: © 2022 by the authors. Licensee MDPI, Basel, Switzerland. This article is an open access article distributed under the terms and conditions of the Creative Commons Attribution (CC BY) license (<https://creativecommons.org/licenses/by/4.0/>).

Keywords: landfill leachate; ammonium; struvite; dolomite; activity ratio diagram

1. Introduction

About 40 percent of the produced solid waste is disposed of in landfills, with another 33 percent disposed of in open dumpsites [1]. The percolation of rainwater through the disposed solid waste generates leachates containing more than 200 potentially toxic compounds [2]. Similarly, the moisture embedded in the solid waste also results in the release of landfill leachates upon waste compaction. If not collected and treated, the leachates pose a severe environmental threat to the adjacent soil and water compartments. Of particular concern is dissolved ammonium, where the un-ionized form (free ammonia) exerts the most toxic effects on aquatic biota [3]. The free ammonia (FA) fraction increases at alkaline pH values such as those present at aged landfills, where ammonium concentration could reach up to 20,000 mg/L [4].

Ammonium is commonly removed from wastewater biologically, through nitrification–denitrification processes. However, the lack of sufficient electron donors in aged landfill leachates could render this process challenging. Moreover, the presence of a high ammonium concentration also exerts negative impacts on biological treatments. Ammonium concentrations below 200 mg/L can be beneficial, whereas greater concentrations may

cause inhibitory effects [5]. Inhibitory effects were reported for ammonium concentrations as low as 1400 mg/L, with the free ammonia species exerting the most inhibitory effects on the methanogens [6–11].

The negative effects of a high ammonium concentration in wastewater on biological treatments can be mitigated by ammonium removal pretreatment. The most commonly used pretreatment methods include ammonia air stripping and ammonium co-precipitation as struvite [12–16]. Struvite is a mineral, with a molecular formula of $\text{NH}_4\text{MgPO}_4 \cdot 6\text{H}_2\text{O}$, that forms naturally in wastewater when magnesium, ammonium, and phosphate concentrations reach saturation level. It is also an effective slow-release fertilizer [17]. Ammonia air stripping technology suffers from the difficulty of operation and potential for ammonia release. It also requires large amounts of alkali and acids to facilitate the ammonia stripping and subsequent wastewater neutralization [18,19]. As for ammonium removal as struvite, most wastewaters contain low concentrations of magnesium and phosphate, relative to ammonium, thus requiring significant amounts of magnesium and phosphate reagents, which renders the treatment costly. To avoid the high costs of the chemical reagents, investigators searched for low-cost alternative sources of magnesium and phosphorous. Alternative phosphorous sources research focused mainly on bone wastes and waste byproducts [19–21]. On the other hand, many sources of low-cost magnesium were identified, such as wood ash, magnesium oxide production byproduct, magnesite, magnesia, dolomite, bittern, and seawater brine [22,23].

The majority of the identified alternative magnesium sources contain significant amounts of calcium, which may negatively impact struvite precipitation. Numerous studies reported on the negative impact of calcium on struvite precipitation; however, most of these studies were focused on phosphorous recovery and the effects of calcium originating from the wastewater [24–27]. The relatively low concentration of calcium in wastewater may have strong impact on the struvite crystal quality, but not necessarily the phosphate removal rates. Conversely, for studies focusing on ammonium removal from landfill leachates, where ammonium concentration could reach up to 20,000 mg/L, the calcium concentration originating from the alternative magnesium source could have significant effects on the ammonium removal rates. Nonetheless, the majority of these studies did not adequately report on the calcium effects originating from the alternative magnesium source [22,28,29]. Regarding the stoichiometric amounts of magnesium needed to precipitate struvite (where magnesium is originating from the alternative magnesium sources), the $\text{Ca}^{2+}:\text{Mg}^{2+}$ molar ratios in the reactors could reach up to 0.48, 0.1, 0.024, 0.098, 1.0, and 0.34 for wood ash, magnesium oxide production byproducts, magnesite, magnesia, dolomite, and bittern, respectively [23,30,31]. The corresponding potential calcium concentration in the reactors for the aforementioned $\text{Ca}^{2+}:\text{Mg}^{2+}$ ratio and ammonium concentration at 20,000 mg/L in the feed could reach 44,417 mg/L.

One of the most promising alternative magnesium sources is bittern. Bittern is a brine residue that forms after the vaporization and crystallization of sodium chloride from sea water or lakes. The magnesium content in bittern is available in the dissolved phase (similar to the presence of magnesium in MgCl_2 salt), which readily enables its reaction with phosphate and ammonium to form struvite. Shin et al. [32] reported comparable phosphorus removal rates from wastewater between bittern (97%) and magnesium chloride salt (99%), but lower ammonium removal rates were achieved by bittern (72%) than by magnesium chloride (83%). The reduced efficiency of bittern for removing ammonium is most likely due to the presence of calcium in the used bittern. The use of bittern to precipitate struvite could also introduce other ions, in addition to calcium, such as chloride, potassium, sodium, and sulfate. However, the use of bittern could be hampered by accessibility or transportation costs in some localities [33]. Conversely, all of the other alternative magnesium sources are present in solid phases. The presence of magnesium in solid phases limits its availability and reactivity to form struvite. However, studies reported on the beneficial use of solid-phase alternative magnesium sources because of

their high alkalinity content which could help mitigate against pH drop upon struvite precipitation [22,28].

This study investigated the effects of calcium on ammonium removal from high strength aged field landfill leachate. Laboratory-scale batch tests were conducted to assess the effects of pH, Mg:NH₄:PO₄ stoichiometric ratios, and Ca²⁺:Mg²⁺ molar ratios on ammonium removal. Magnesium chloride salt was used as a model dissolved magnesium source, whereas different compounds derived from dolomite (CaMg(CO₃)₂) were used as model solid-phase magnesium sources. X-ray powder diffraction and activity ratio diagrams were used to delineate the removal mechanisms and assess the stability of struvite in the presence of competing solid phases.

2. Material and Methods

2.1. Materials

The leachate was collected from a municipal solid waste landfill in Tripoli, Lebanon (34°27'21.539" N, 35°50'22.559" E). The landfill is located along the Mediterranean coastline, and it covers an area of 60,000 m². It started operations in 1980 and was planned to close in 2012; however, due to a lack of alternatives, it was still receiving an average of 450 tons/day, as of 2020 [34]. A large volume of the leachates was collected, mixed, and centrifuged at 13,000 rpm (19,685 × g) for 30 min before characterization. The centrifuged samples were then stored in a fridge at 4 °C. The samples needed for the set experiments were allowed to reach room temperature for one hour before use. The dolomite was obtained from a local sand supplier in North Lebanon. It was first sieved using a sieve #40 to remove debris; then, it was manually grinded and sieved using sieve #200 and mechanical sieve shaker. It was then stored in plastic bags until used. Tri-sodium phosphate (Na₃PO₄·12H₂O) was used as the phosphate source. Magnesium chloride (MgCl₂) and calcium chloride (CaCl₂) were used in batch experiments to assess the efficacy of the magnesium source and effects of calcium on struvite precipitation, respectively. Hydrochloric acid (HCl) and sodium hydroxide (NaOH) were used to adjust pH. All chemicals used were of analytical grade, and they were obtained from Fisher Scientific (Hampton, NH, USA).

2.2. Struvite Precipitation Batch Tests

For the struvite batch precipitation tests, 50 mL of centrifuged leachate was added to a beaker containing a magnetic stirring rod, which was then placed on a LabTech LMS-1003 hot plate magnetic stirrer. The phosphate, magnesium, and calcium (when applicable) sources were then added to the leachates. The reactants were mixed for 30 min, while pH was controlled at a set value ±0.05 pH units, using HCl and NaOH, and monitored using a WPA CD 500 pH meter (Cambridge, UK). After mixing for a set reaction time, the mixture was allowed to settle for 15 min, then centrifuged at 13,000 rpm (19,685 × g) for 30 min, before analysis. Similar studies reported mixing times less than or equal to 30 min [18,19,21,28,35,36]. Resulting precipitates were dried in a desiccator and stored for analysis. All experiments were performed in triplicate at a room temperature of 20 ± 2 °C. The supernatants were analyzed for NH₃, PO₄³⁻, Mg²⁺, and Ca²⁺, whereas the precipitates were analyzed for solid phases using XRPD.

2.3. Analytical Methods

A Hach DR3900 spectrophotometer was used for all spectrophotometry analyses procedures, and a Hach DRB200 digester block was used for the analytical procedures requiring digestion. Ammonia nitrogen NH₃-N was measured using the Hach salicylate method 10031. Chemical oxygen demand (COD) was measured using the Hach method 8000 with high-range digestion vials. Biochemical oxygen demand (BOD) was conducted as per Standard Method 5210B. Total organic carbon (TOC) was measured using Hach method 10128. Phosphate was measured using Hach orthophosphate method 8048; Mg²⁺ and Ca²⁺ and other heavy metals were measured using a PerkinElmer PinAAcle 900H atomic absorption spectrophotometer. Chloride and sodium ions were quantified by ion

chromatography, using an 882 Compact IC Plus (Metrohm, Herisau, Switzerland) equipped with a chemical suppressor module and conductivity detector. Chloride ions were detected after separation using a Metrosep A supp 5 column (250 × 4 mm), with an eluent consisting of 3.5 mmol·L⁻¹ sodium carbonate and 1 mmol·L⁻¹ sodium hydrogen carbonate, as well as an eluent flow rate of 0.7 mL·min⁻¹ and suppressor regenerant of 0.1 mol·L⁻¹ sulfuric acid. Sodium ions were detected after separation using a Metrosep C4 column (150 × 4.0 mm), with an eluent consisting of 4 μmol·L⁻¹ nitric acid (69%) at a flow rate of 0.9 mL·min⁻¹. Injection volumes of 20 μL were used for all measurements. Calcinations were performed in a Nabertherm GmbH burnout furnace L3/12. Centrifugation was performed in a TermoScientific fixed-bucket centrifuge.

Check standards were performed routinely, as well as matrix spikes, in order to check the accuracy of the instruments and analytical procedures and ensure that there were no interferences affecting the results. Three control experiments were conducted to check whether any of the ammonium removal was not due to struvite precipitation. The first experiment was conducted without adding any reagents to the leachate. In the second experiment, only dolomite was added to the leachate; in the third experiment, only Na₃PO₄·12H₂O was added. All control experiments were conducted at a reaction time of 30 min, using a pH value of 9.5 and Mg²⁺:NH₄⁺:PO₄³⁻ molar ratio of 1.25:1:1.25. No ammonium removal was observed in all control experiments.

2.4. X-ray Powdered Diffraction

The solid phases were analyzed using a Bruker D8 Advance X-Ray diffractometer. Diffractometry was conducted at 40 kV and 40 mA using a Cu tube. Data were collected in the 2θ range of 5° to 65° using 3080 steps, with 0.2 s between each step. Qualitative analysis of the obtained patterns was performed in reference to the International Center of Diffraction Data (ICDD) database, using the DIFFRAC.EVA software Version 4.2.1.

2.5. Activity Ratio Diagram Modeling

Activity ratio diagrams were constructed to identify the solid phases controlling the solubility of the major ions responsible for the removal of ammonium from the leachate [37–39]. The chemical database of the geochemical speciation model, Visual Minteq, was used to plot the activity ratios of pertinent solid phases as a function of various ions [40]. The Truesdell–Jones equation was used to calculate the activity coefficients for all species, except for phosphate, due to the lack of pertinent thermodynamic data [41]. The Davies equation was used to calculate the activity coefficient of phosphate.

3. Results and Discussion

3.1. Leachate Characterization

The characterization results of the untreated landfill leachate are presented in Table 1.

Table 1. Characterization of the untreated leachate.

Parameter	Value (mg/L)
pH	8.26
BOD ₅	1130
COD	12,050
TOC	3400
Cl ⁻	2676.4
NO ₃ ⁻	2.5
PO ₄ ³⁻	57.6
SO ₄ ²⁻	47.7
Ca ²⁺	58.78
K ⁺	2483
Mg ²⁺	31.82
Na ⁺	2000

Table 1. *Cont.*

Parameter	Value (mg/L)
NH ₄ ⁺	4584
Al	3.38
As	0.062
Cd	<0.005
Cr	1.77
Cu	0.536
Hg	0.007
Pb	0.127
Zn	0.430

The measured BOD₅/COD ratio and pH of the leachate were approximately 0.093 and 8.26, respectively, indicating that the landfill is classified as mature and in the methanogenic phase [2,42,43]. The landfill leachate had an average ammonium concentration of about 4583 mg/L, which is greater than the typical range of values of ammonium in landfill leachates of 500–2000 mg/L NH₃-N [2]. The free ammonia (FA) fraction in the leachates at a pH of 8.26 was calculated at approximately 6.7% or 290 mg/L, at a temperature of 20 °C [44]. This value is much greater than the concentrations of free ammonia reported to cause inhibition in biological treatments. For example, Liu et al. [5] reported a free ammonia inhibition of 40% on denitrifiers at a FA concentration of 16 mg NH₃/L and 80% inhibition on methanogens at a FA concentration of 40 mg NH₃-N/L. The characterization results also showed the presence of low concentrations of calcium and magnesium at approximately 58.8 and 32 mg/L, respectively, as compared to values reported in the literature. The concentration of phosphate at 57.6 mg/L was relatively greater than that of the average value of 6 mg/L reported in landfill leachates. The concentrations of cadmium and lead at <0.005 and 0.127 mg/L, respectively, were close to the average reported values at 0.005 and 0.09 mg/L, respectively. However, the concentrations of copper and chromium at 0.536 and 1.77 mg/L, respectively, were relatively greater than the average values cited in the literature at 0.065 and 0.28 mg/L, respectively [2]. The relatively low concentrations of the heavy metals in the leachate could be due to the alkaline pH of the leachate, as metal cations have lower solubility at high pH. As for arsenic, it is expected to be present in an anionic form, where its low concentration could indicate a trace level presence or strong arsenic sorptive affinity of the solid waste constituents. The presence of chromium and copper at concentrations relatively greater than the average values reported at landfills could indicate the potential sources of contamination and lack of apparent sequesters.

3.2. Ammonium Removal Using Magnesium Chloride Salt

Batch test experiments were conducted to remove ammonium by struvite precipitation using magnesium and phosphate salt. These experiments were conducted to determine the optimal Mg²⁺:NH₄⁺:PO₄³⁻ molar ratio and pH for ammonium removal from the leachate, as well as to use the test results as a benchmark for the experiments using alternative magnesium sources. All tested conditions are shown in Table 2, and the resulting concentrations of Mg²⁺, NH₄⁺, PO₄³⁻, and Ca²⁺ are shown in Table S1.

Table 2. Experimental conditions tested.

Experiment No.	Mg ²⁺ :NH ₄ ⁺ :PO ₄ ³⁻ Molar Ratios	Mg ²⁺ Source	Ca ²⁺ :Mg ²⁺ Molar Ratio	Ca ²⁺ Source	pH
1	1:1:1	MgCl ₂	0	-	9.5
2	1.25:1:1	MgCl ₂	0	-	9.5
3	1:1:1.25	MgCl ₂	0	-	9.5
4	1.25:1:1.25	MgCl ₂	0	-	9.5

Table 2. Cont.

Experiment No.	Mg ²⁺ :NH ₄ ⁺ :PO ₄ ³⁻ Molar Ratios	Mg ²⁺ Source	Ca ²⁺ :Mg ²⁺ Molar Ratio	Ca ²⁺ Source	pH
5	1.25:1:1.25	MgCl ₂	0	-	8.5
6	1.25:1:1.25	MgCl ₂	0	-	10.5
7	1.25:1:1.25	MgCl ₂	0.1	CaCl ₂	9.5
8	1.25:1:1.25	MgCl ₂	0.2	CaCl ₂	9.5
9	1.25:1:1.25	MgCl ₂	0.5	CaCl ₂	9.5
10	1.25:1:1.25	MgCl ₂	1.0	CaCl ₂	9.5
11	1.25:1:1.25	CaMg(CO ₃) ₂	1.0	CaMg(CO ₃) ₂	9.5
12	1.25:1:1.25	MgO	1.0	CaCO ₃	9.5
13	1.25:1:1.25	MgO	1.0	CaO	9.5

3.2.1. Effects of Molar Ratios

The effects of the molar ratios of phosphate and magnesium to ammonium on the removal rates of ammonium were investigated for molar ratios ranging between 1 and 1.25 (Table 2). Equimolar ratios of Mg²⁺:NH₄⁺:PO₄³⁻ are needed to form struvite, but the presence of other constituents in the leachates can reduce the precipitation efficiency, which results in a need for higher magnesium and phosphate molar ratios. The experiments were conducted using a pH value of 9.5.

The results of Exp.1, with Mg²⁺:NH₄⁺:PO₄³⁻ molar ratios of 1:1:1, indicated an ammonium removal rate of approximately 81%, with phosphate and magnesium removal rates of 82% and 99.9%, respectively (Figure 1a). It appears that magnesium dosage was limiting, considering that it was nearly fully exhausted. It also appears that using Mg²⁺ and PO₄³⁻ at equal molar ratios to ammonium might not be optimal for the removal of ammonium. The incomplete ammonium removal and high residual phosphate concentration in the supernatant indicate the potential for improvement in ammonium removal by increasing the magnesium dosage. The need for molar ratios of magnesium and phosphate to ammonium that are greater than 1.0 is attributed to the formation of insoluble and, possibly, amorphous magnesium and phosphate compounds, other than struvite, such as Mg₃(PO₄)₂ and Ca₃(PO₄)₂ [19,45–48]. For example, Huang et al. [49] showed that, as the ratio of Ca(OH)₂ to NaOH (used to adjust pH) increased in the range of 0:1–1:1, ammonium removal efficiency decreased from 85% to 75%. Increasing magnesium dosage alone (1.25:1:1) resulted in an increase in ammonium removal rate to approximately 92%, with phosphate and magnesium removal rates at approximately 99.7% and 96%, respectively. On the other hand, increasing the phosphate dosage (PO₄³⁻:NH₄⁺) alone to 1.25:1 (Exp.3) resulted in an ammonium removal efficiency of approximately 83%. The corresponding removal rates of magnesium and phosphate were approximately 99.9% and 73%, respectively. This indicates that the excess amounts of added phosphate remained in the solution. When both magnesium and phosphate dosages were increased to 1.25:1, with respect to ammonium (Exp.4: 1.25:1:1.25), the ammonium removal rate increased to approximately 97%, with magnesium and phosphate removals of 99.9% and 90%, respectively. Finally, considering the concern regarding the presence of significant amounts of residual phosphate in the treated leachates, it may be preferable to select the treatment condition with a Mg²⁺:NH₄⁺:PO₄³⁻ molar ratio of 1.25:1:1 for application in the field [50]. Even though this condition did not achieve the greatest ammonium removal rate (92%), it did achieve the greatest phosphate removal rate of about 99.7%. The residual ammonium concentration in the treated leachate may be less of a concern than the amount of residual phosphate.

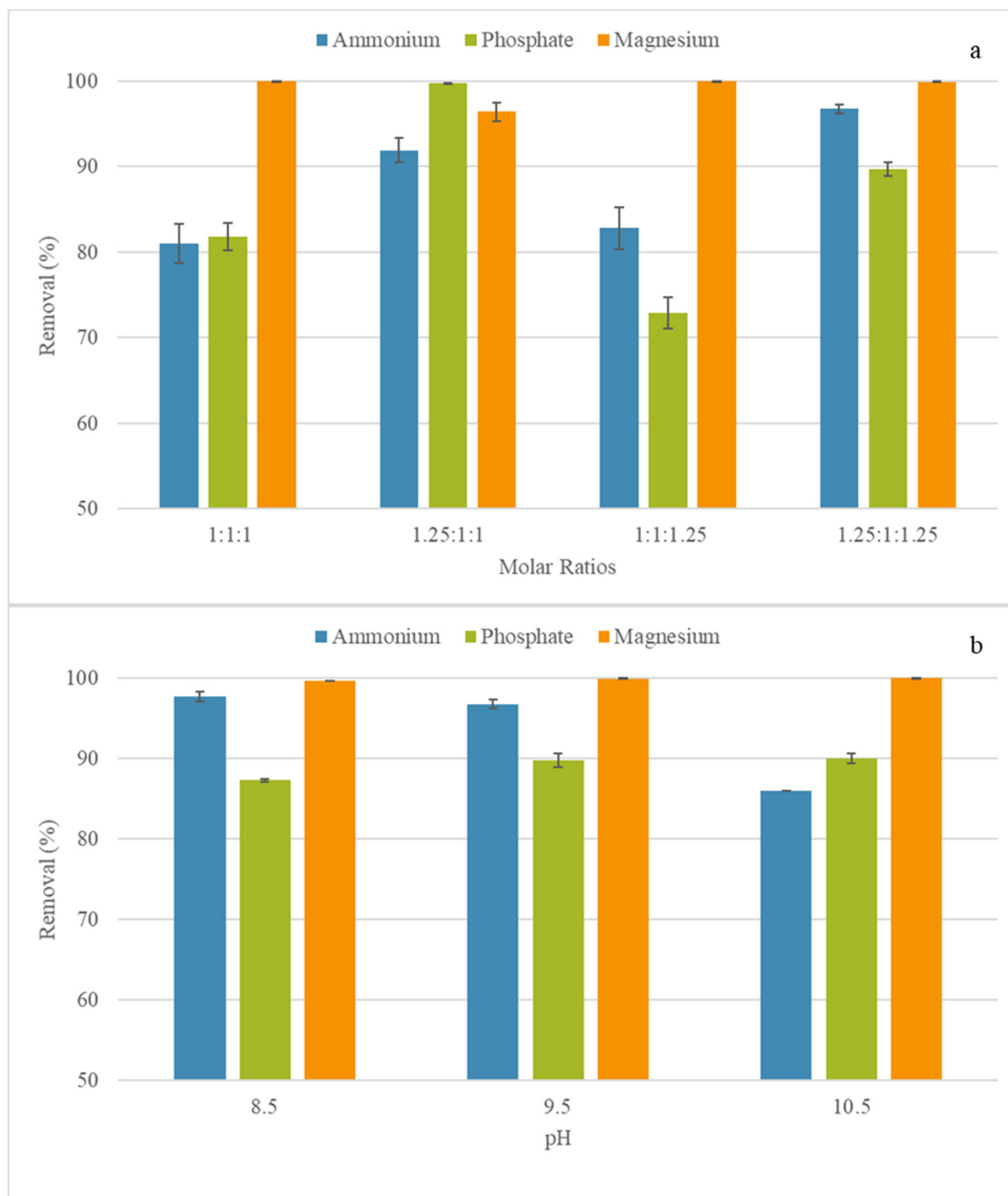


Figure 1. Ammonium, phosphate and magnesium removal rates vs. ($\text{Mg}^{2+}:\text{NH}_4^+:\text{PO}_4^{3-}$) molar ratios at pH = 9.5 (a) and vs. pH at molar ratios of 1.25:1:1.25 (b). The error bars represent \pm one standard deviation for three replicate experiments.

3.2.2. Effects of pH

The effects of pH on ammonium removal were investigated using pH values of 8.5, 9.5, and 10.5, as well as $\text{Mg}^{2+}:\text{NH}_4^+:\text{PO}_4^{3-}$ molar ratios of 1.25:1:1.25 (Figure 1b). The results at a pH of 9.5 showed ammonium removal efficiency of approximately 97%. When pH was increased to 10.5, ammonium removal efficiency decreased to approximately 86%, whereas, when pH decreased to 8.5, ammonium removal remained roughly the same at about 98%. As pH increases (mainly above 9.5–10.0), ammonium solubility, with respect to struvite, increases, which could result in an increase in ammonium concentration in the solution [18,51]. In addition, high pH values could promote magnesium hydration,

resulting in the formation of brucite $\text{Mg}(\text{OH})_2$, which could scavenge magnesium [52]. This may explain the drop in ammonium removal efficiency at a pH of 10.5. Similarly, lower pH values increase ammonium solubility, with respect to ammonium. However, the increase in ammonium solubility upon pH change from 9.5 to 8.5 was not significant. Actually, the ammonium removal rate remained essentially the same. Other studies reported optimal ammonium removal by struvite precipitation in the pH range of 8.5–10 [48,53,54].

3.3. Ammonium Removal Using Dolomite-Derived Compounds

Dolomite was pre-treated thermally to increase its activity as an alternative magnesium source. The thermal treatment of dolomite under a CO_2 atmosphere and 750°C resulted in the formation of magnesium oxide (MgO) and calcite (CaCO_3). On the other hand, the thermal treatment under atmospheric conditions and a temperature of 950°C resulted in the formation of MgO and lime (CaO) (Supplementary Material) [22,55,56]. In addition to the activation of the magnesium content, the thermal treatment of dolomite under the two different atmospheres also resulted in the formation of two different calcium sources, i.e., calcite and lime. Raw, CO_2 -calcined, and air-calcined dolomite were used to investigate the removal of ammonium from the landfill leachates. The $\text{Mg}^{2+}:\text{NH}_4^+:\text{PO}_4^{3-}$ molar ratios and pH were set at 1.25:1:1.25 and 9.5, respectively. These conditions were selected to enable a performance comparison with the test results, using magnesium chloride salt under optimized ammonium removal conditions.

The batch test experiment using raw dolomite resulted in an ammonium removal rate of approximately 17% (Figure 2). When CO_2 -calcined dolomite was used, the ammonium removal rate increased to approximately 37%, whereas, when air-calcined dolomite was used, the ammonium removal rate increased to approximately 55%. The removal rate of magnesium for all three conditions was approximately 100%. Conversely, the removal rates of phosphate were approximately 14%, 71%, and 58% for the raw dolomite, CO_2 -calcined dolomite, and air-calcined dolomite, respectively.

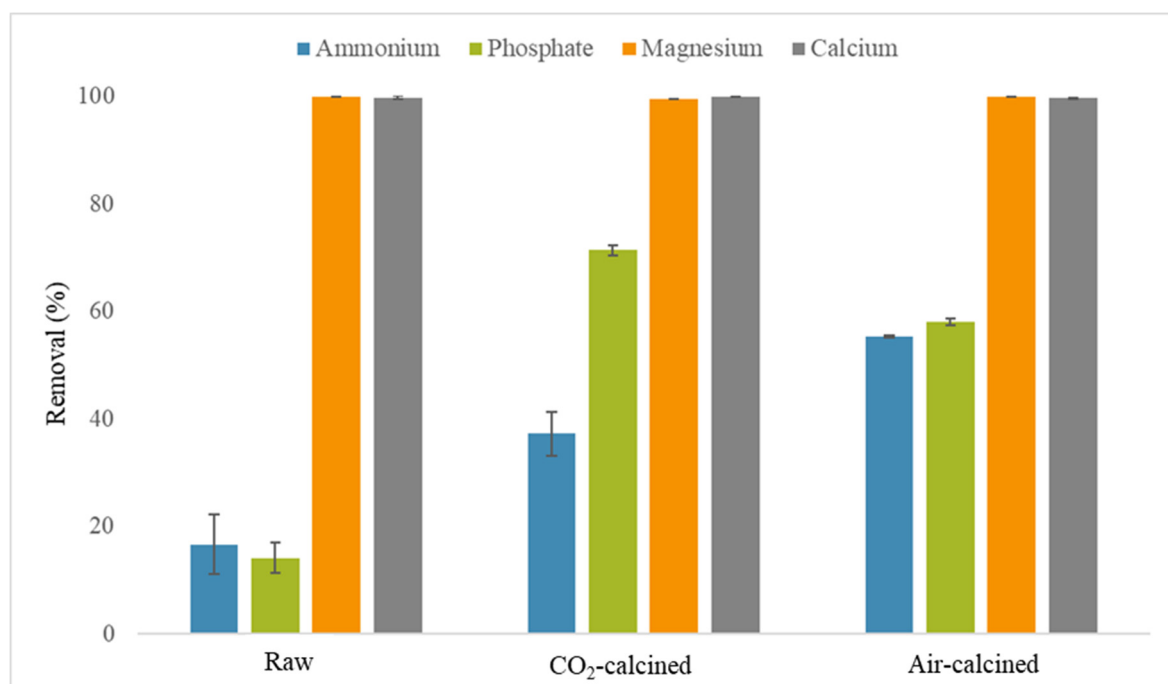


Figure 2. Ammonium, phosphate, magnesium, and calcium removal rates for the different treatment conditions using dolomite ($\text{Mg}^{2+}:\text{NH}_4^+:\text{PO}_4^{3-} = 1.25:1:1.25$; pH = 9.5). The error bars represent \pm one standard deviation for three replicate experiments.

It appears that magnesium was not readily available, as evidenced by the high concentration of dissolved phosphate and ammonium in the supernatant. It also appears that calcium was not readily available, as evidenced by the high concentration of phosphate in the supernatant. Greater ammonium removal rates were achieved by the air-calcined dolomite than by the CO₂-calcined dolomite. Conversely, greater phosphate removal rates were achieved by the CO₂-calcined dolomite than by the air-calcined dolomite. This could indicate that calcium was more available or active in the CO₂-calcined dolomite (as CaCO₃) than the air-calcined dolomite (as CaO), assuming that the residual phosphate was mostly removed by calcium. For field application, the air-calcined dolomite seems preferable, considering the higher ammonium removal rates and lower phosphate removal rates. Greater magnesium concentrations could be used to simultaneously increase the ammonium and phosphate removal rates. Alternatively, the supernatant could be reused in new precipitation experiments via the addition of new activated dolomite, in order to remove the residual ammonium and phosphate as struvite.

3.4. Effects of Calcium

In order to investigate the role of calcium in the decrease of ammonium removal rates by the dolomite-derived compounds, experiments were conducted to precipitate struvite from the landfill leachates using magnesium and phosphate salts in the presence of calcium salt. The results are shown in Figure 3. The addition of calcium, in the form of calcium salt, resulted in a decrease in the efficiency of ammonium removal. The ammonium removal rates were approximately 97%, 97%, 95%, 93%, and 70% for the calcium-to-magnesium molar ratios of 0, 0.1, 0.2, 0.5, and 1.0, respectively. Minimal effects were observed for calcium-to-magnesium ratios up to 0.5 at tested conditions. However, a significant reduction in the ammonium removal rate at 70% was observed when the calcium-to-magnesium molar ratio increased to 1.0. Greater ammonium removal rates were achieved by the magnesium salt, as compared to the corresponding removal rates by activated dolomite, for a similar Ca²⁺:Mg²⁺ molar ratio of one (70% versus 55%). This may indicate that dissolved alternative magnesium sources can outperform the solid-phase alternative magnesium sources for ammonium removal from wastewater, realizing that calcium was likely more available as salt than calcite or lime. The reduced efficiency of the solid-phase alternative magnesium sources could be due to the unavailability of magnesium during the co-precipitation reaction. The reduced efficiency of the solid-phase alternative magnesium sources may outweigh its added benefit, mitigating against the drop in pH upon struvite precipitation.

The formation of calcium phosphate solid phases is thermodynamically favorable under the experimental conditions, where calcium is expected to react with the added phosphates and potentially hinder the formation of struvite. However, the removal of significant amounts of ammonium indicated the formation of struvite, because struvite is the only route for ammonium removal in our system. Studies have reported that hydroxyapatite is thermodynamically stable at equilibrium, and it could uptake added phosphates as per its stoichiometry; however, that was not the case in this study, as evidenced by the high concentration of phosphate in the supernatant [26,27]. The order of the formation of the mineral phases, duration of the co-precipitation reactions experiments, and concentration of competing ions may have an impact on the resulting solid phases [25,57,58].

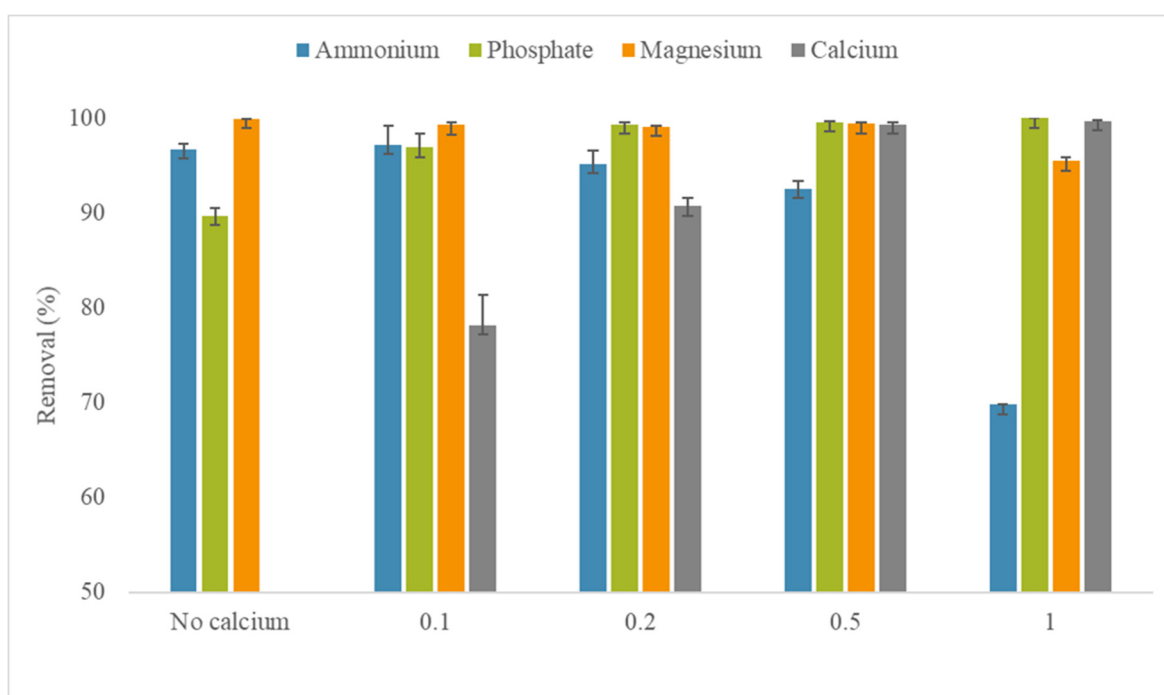


Figure 3. Ammonium, phosphate, magnesium, and calcium removal rates for the calcium salt source effects experiments ($Mg^{2+}:NH_4^+:PO_4^{3-} = 1.25:1:1.25$, pH = 9.5). The error bars represent \pm one standard deviation for three replicate experiments.

3.5. XRD Results

XRPD analysis was used to identify the solid phases that formed during the coprecipitation reactions and delineate the removal mechanisms of ammonium from the leachates. The XRPD patterns for the precipitates of the experiments using magnesium chloride salt are shown in Figure 4a. The results indicated the presence of struvite with characteristic peaks at 15.787° , 20.839° , and 30.573° (PDF 04-010-2533). Struvite is the major sequester of ammonium in the presence of magnesium and phosphate, and it is expected to be the only mechanism responsible for the removal of ammonium from the leachate. The XRPD patterns also indicated the presence of halite (NaCl), with characteristic peaks at 31.692° , 45.449° , and 56.477° (PDF 00-005-0628). Sodium is present due to the addition of sodium phosphate as the phosphate source, whereas chloride is present due to the presence of chloride in the leachates, as well as the added hydrochloric acid and calcium chloride. The absence of any crystalline calcium solid phases in the XRPD pattern, pertaining to the experiment with the added calcium chloride, is noteworthy (Figure 3a). The added calcium could be encapsulated in amorphous solid phases, as indicated by the amorphous hump in the corresponding XRPD pattern [27].

The XRPD analyses of the precipitates for the thermally-treated dolomite experiments clearly indicated the presence of struvite, with characteristic peaks at 15.787° , 20.839° , and 30.573° (PDF 04-010-2533) (Figure 4b). This indicates that ammonium was removed from the leachate by sequestration in struvite. The precipitates of the CO_2 calcination experiment showed characteristic peaks of calcite and periclase at 23.07° , 29.454° , 48.578° (PDF 00-024-0027), and 42.855° , 62.215° (PDF 01-071-1176), respectively, which indicates that these phases did not dissolve or hydrate completely. For the experiment with raw dolomite, XRPD analysis detected major peaks of dolomite at 30.938° , 41.127° , and 56.477° (PDF 00-036-0426), which indicated that dolomite was not significantly destabilized (XRPD patterns of raw and calcined dolomite are shown in Figure S1). No struvite peaks were identified for the raw dolomite experiments, which could be due to the presence of struvite at concentrations below the detection limit of the XRPD.

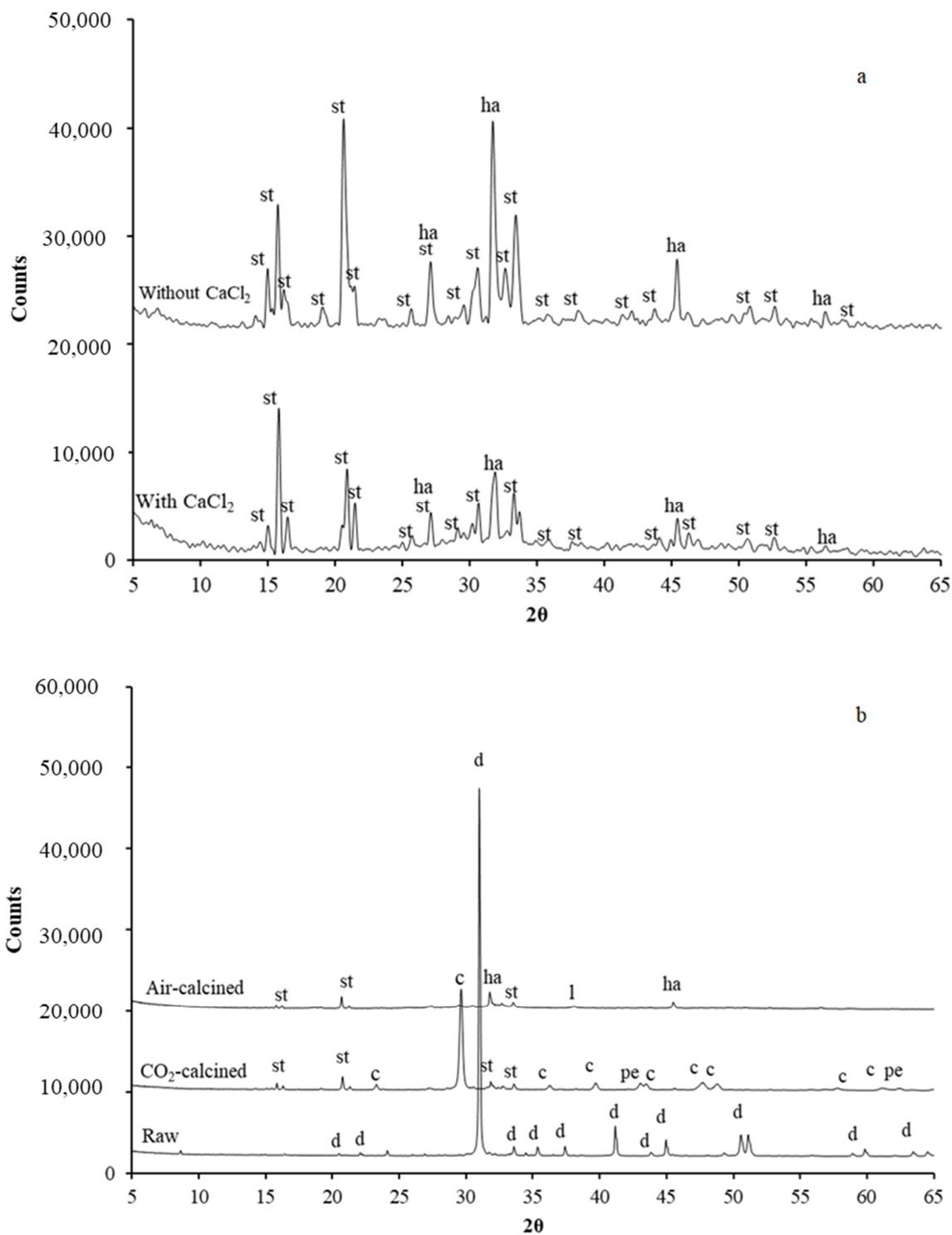


Figure 4. XRPD of the precipitates for the ($Mg^{2+}:NH_4^+:PO_4^{3-} = 1.25:1:1.25$; pH = 9.5) experiments using $MgCl_2$, $Na_3PO_4 \cdot 12H_2O$, and $CaCl_2$ as magnesium, phosphate, and calcium sources, respectively (a). And the experiments using dolomite under different pretreatment conditions (b). d = dolomite; c = calcite; pe = periclase; l = lime; po = portlandite; st = struvite; ha = halite.

Finally, no calcium phosphate or magnesium phosphate solid phases were identified in the XRPD analyses for all experimental conditions. This could be due to the instability of these phases, their presence at concentrations below the detection limits of the XRPD, or their presence as amorphous solid phases.

3.6. Activity Ratio Diagrams

Activity ratio diagrams were constructed to further delineate the ammonium removal mechanisms and investigate the stability of the solid phases controlling the solubility of ammonium and phosphate. The probable solid phases controlling the solubility of ammonium, magnesium, phosphate, and calcium are listed in Table 3. The activity ratio diagrams could qualitatively indicate the behavior of the system, especially in the presence of competing ions that could interfere with the formation of struvite and, thus, removal of ammonium. The activity of the phosphate is of particular concern, because the magnesium phosphate and calcium phosphate phases could compete with struvite for its sequestration. The thermodynamic data of the solid phases were obtained from Visual Minteq [40].

Table 3. Precipitation reactions used in the construction of the activity ratio solubility diagrams.

Solid Phase			Log k
Struvite	=	$Mg^{2+} + NH_4^+ + PO_4^{3-}$	-13.26
$Ca_3(PO_4)_2$ am1	=	$3Ca^{2+} + 2PO_4^{3-}$	-25.5
$Ca_3(PO_4)_2$ am2	=	$3Ca^{2+} + 2PO_4^{3-}$	-28.25
$Ca_3(PO_4)_2$ (beta)	=	$3Ca^{2+} + 2PO_4^{3-}$	-28.92
$Ca_4H(PO_4)_3 \cdot 3H_2O$	=	$4Ca^{2+} + H^+ + 3PO_4^{3-} + 3H_2O$	-47.95
$CaHPO_4$	=	$Ca^{2+} + H^+ + PO_4^{3-}$	-19.275
Hydroxyapatite + H^+	=	$5Ca^{2+} + 3PO_4^{3-} + H_2O$	-44.333
$Mg_3(PO_4)_2$	=	$3Mg^{2+} + 2PO_4^{3-}$	-23.28
$MgHPO_4 \cdot 3H_2O$	=	$Mg^{2+} + PO_4^{3-} + H^+ + 3H_2O$	-18.175

The activity ratios of the solid phases controlling phosphate solubility are plotted versus magnesium concentration, as shown in Figure 5a. The ammonium and calcium concentrations used in the construction of the diagram were the average values obtained in this study. The plots show that the solubility of phosphate at equilibrium and in the presence of calcium is controlled by hydroxyapatite (highest activity ratio line), independent of the concentration of magnesium. However, hydroxyapatite was not identified in the XRPD analysis, and its formation could be kinetically delayed. In the absence of hydroxyapatite, phosphate solubility is controlled by other calcium phosphate phases, except for magnesium concentrations greater than approximately 10^{-2} M, where phosphate solubility is controlled by struvite. If the concentration of calcium is increased by about two orders of magnitude (0.2 M), as it was at the start of the experiment for the $Ca^{2+}:Mg^{2+}$ ratio of 1.0, additional calcium phosphate phases activity ratio lines move above the struvite one and appear to control the solubility of the phosphate (Figure S2). The order of the activity ratio lines do not change appreciably when the ammonium concentration is concurrently increased to 0.2 M.

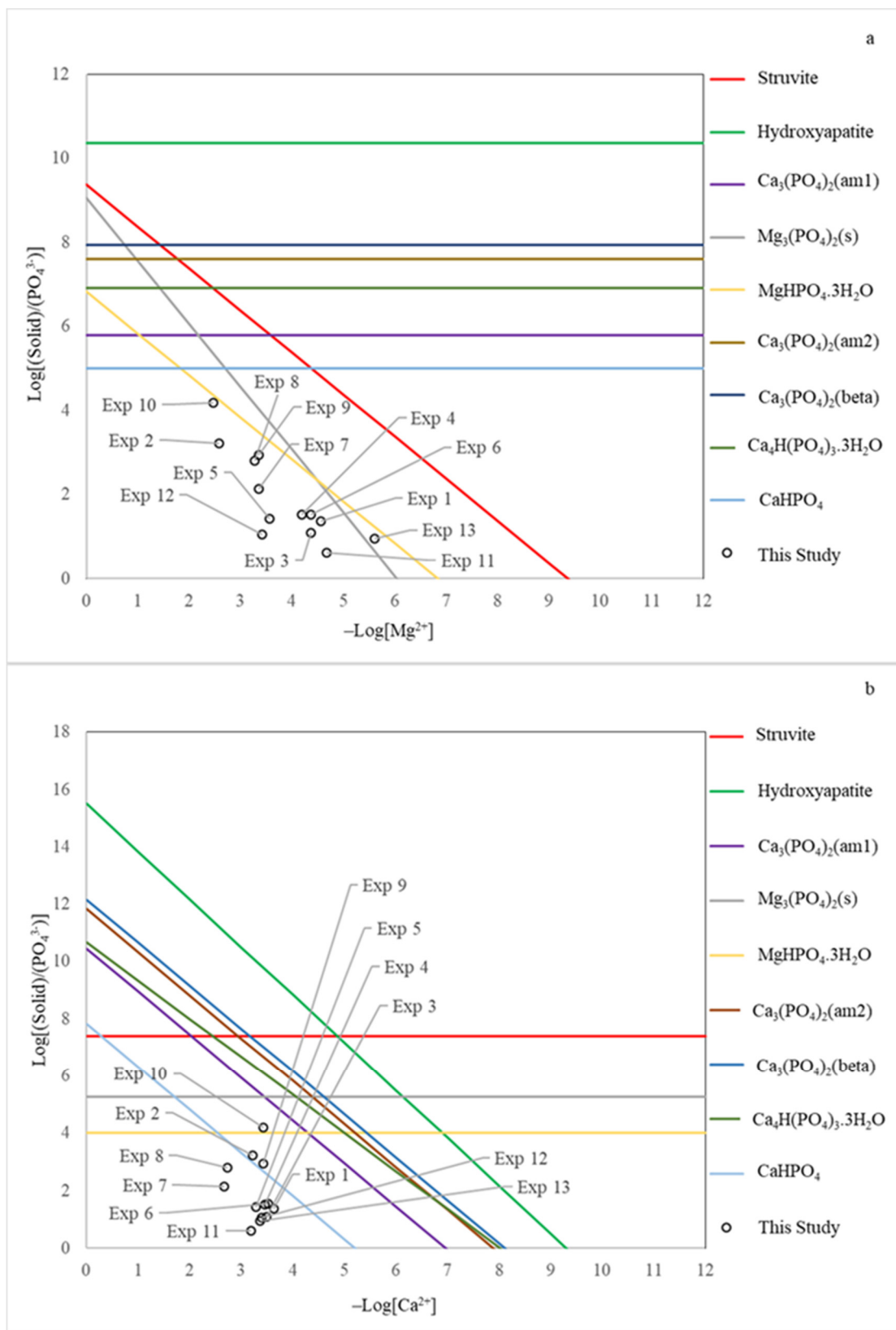


Figure 5. Activity ratio diagrams for: (a) PO_4^{3-} solid phases vs. Mg^{2+} . $\text{pH} = 9.5$, $\text{NH}_4^+ = 0.0527 \text{ M}$, $\text{Ca}^{2+} = 0.001 \text{ M}$; (b) PO_4^{3-} solid phases vs. Ca^{2+} . $\text{pH} = 9.5$, $\text{NH}_4^+ = 0.0527 \text{ M}$, $\text{Mg}^{2+} = 0.0026 \text{ M}$.

According to the Gay-Lussac-Ostwald (GLO) step rule, if several solid phases can potentially form with a given ion, the first solid phase to form is the one for which the activity ratio is nearest above the initial concentration. The remaining potential solid phases will form in the order of increasing activity ratio, with the rate of formation of the solid phases decreasing with increasing activity ratios. However, any solid phase can be maintained indefinitely [39]. Consequently, and as per the GLO step rule, the first phosphate solid phases that are expected to form at a magnesium concentration less than approximately 10^{-2} M are magnesium phosphates, $Mg_3(PO_4)_2$, and $MgHPO_4 \cdot 3H_2O$. However, phosphate solubility is ultimately controlled by calcium phosphate phases, with a struvite activity ratio line located between the magnesium phosphate and calcium phosphate activity ratio lines. If calcium concentration is exhausted or unavailable, then phosphate solubility is first controlled by magnesium phosphate solid phases and then by struvite. The $Mg_3(PO_4)_2$ and $MgHPO_4 \cdot 3H_2O$ solid phases were not identified in the XRPD analysis, but that does not necessarily mean that they did not form. It is speculated that these phases are transient ones, and they could have formed (even as amorphous ones); however, as the magnesium and phosphate concentrations decreased, due to the formation of the aforementioned magnesium phosphate phases, the equilibrium shifted towards the formation of struvite and dissolution of the magnesium phosphate phases. The significant removal of calcium could be due to the formation of amorphous calcium phosphate phases [27].

The experimental data in this study were plotted at or below the activity ratio lines corresponding to $Mg_3(PO_4)_2$ and $MgHPO_4 \cdot 3H_2O$. It appears that the presence of the data points at and below the $Mg_3(PO_4)_2$ and $MgHPO_4 \cdot 3H_2O$ activity ratio lines did not preclude the formation of struvite. The experimental data of other struvite co-precipitation studies (where calcium and magnesium concentrations were available) were also plotted within the same data cluster [19,35,59]. Liu and Wang [26] reported that struvite nucleate ahead of magnesium phosphate phases and would later transform to magnesium phosphate under excessive magnesium concentration. The later transformation of struvite to magnesium phosphate does not appear to have occurred in this study, as evidenced by the identification of struvite using XRPD analysis and significant removal rates of ammonium. However, this does not contradict the GLO rule, as any formed solid phase can be maintained indefinitely.

The concentration of ammonium was fixed during the construction of the diagram in Figure 5a as the average of the values obtained in this study. Other assumptions about ammonium concentration could be made; for example, a decrease in the concentration of ammonium by one order of magnitude will result in a downward shift in the struvite activity ratio line of one order of magnitude, placing the activity ratio line of struvite closer to that of magnesium phosphate. On the other hand, an increase in the concentration of ammonium by one order of magnitude will result in an upward shift of the struvite activity ratio line of one order of magnitude. The downward shift will move equilibrium toward the formation of struvite close to and ahead of $Mg_3(PO_4)_2$, whereas the upward shift will have no effects on the order of formation between that of the struvite and magnesium phosphate solid phases.

The plot of the activity ratio for the solid phases controlling the phosphate concentration versus the concentration of calcium are shown in Figure 5b. At equilibrium, the concentration of phosphate is expected to be controlled by struvite at calcium concentration less than approximately 10^{-5} M and hydroxyapatite at calcium concentrations greater than approximately 10^{-5} M. Assuming that the formation of hydroxyapatite could be kinetically delayed for the duration of the experiment, the practical range of calcium concentration that struvite controls phosphate solubility could be extended to less than approximately $10^{-3.3}$ M. At calcium concentrations greater than $10^{-3.3}$ M, the solubility of phosphate is first controlled by struvite and later controlled by calcium phosphate phases. If struvite nucleates first, then it has the potential to remain stable indefinitely, as per the GLO rule, which could explain its presence in the precipitates. Increasing the concentration of magnesium by about two orders of magnitude (0.2 M), as it was at the start of the experiment, will

result in an upward shift of the struvite activity ratio line by two orders of magnitude, thus practically extending the range of calcium concentration, where phosphate concentration will be mainly controlled by struvite (Figure S3).

4. Conclusions

The experimental data showed that increasing the molar ratio of magnesium to ammonium and phosphate during the co-precipitation treatment resulted in a relatively lower ammonium removal rate and lower residual phosphate concentration in the treated leachate. This treatment option appears to be preferable to the one with a higher ammonium removal rate and higher residual phosphate concentration in the treated leachate, due to concerns regarding phosphorus discharge. The thermal treatment of dolomite significantly increased its capacity to remove ammonium from landfill leachates. However, greater ammonium removal rates were achieved by magnesium salt, as compared to the corresponding removal rates of dolomite-derived compounds for a similar $\text{Ca}^{2+}:\text{Mg}^{2+}$ molar ratio. This may indicate that dissolved alternative magnesium sources can outperform solid-phase alternative magnesium sources for ammonium removal from wastewater. The reduced efficiency of the solid-phase alternative magnesium sources could be due to the unavailability of magnesium during the co-precipitation reaction. Future studies could focus on the assessment of the produced precipitate as a fertilizer or soil amendment, including the impact of calcium presence. The new insights into the stability of struvite and other phosphate sequestering solid phases could be used advantageously to design better ammonium and phosphate removal and recovery systems via struvite precipitation.

Supplementary Materials: The following supporting information can be downloaded at: <https://www.mdpi.com/article/10.3390/w14121933/s1>, Figure S1: X-Ray Diffractograms of the products of the different dolomite thermal pretreatment processes. d = dolomite $\text{MgCa}(\text{CO}_3)_2$; c = calcite CaCO_3 ; pe = periclase; MgO ; l = lime CaO ; po = portlandite $\text{Ca}(\text{OH})_2$; Figure S2. Activity ratio diagram for PO_4^{3-} solid phases vs. Mg^{2+} . $\text{pH} = 9.5$, $\text{NH}_4^+ = 0.0527 \text{ M}$, $\text{Ca}^{2+} = 0.2 \text{ M}$; Figure S3. Activity ratio diagram for PO_4^{3-} solid phases vs. Ca^{2+} . $\text{pH} = 9.5$, $\text{NH}_4^+ = 0.0527 \text{ M}$, $\text{Mg}^{2+} = 0.2 \text{ M}$; Table S1: The final concentrations of Mg^{2+} , NH_4^+ , PO_4^{3-} , and Ca^{2+} , pertaining to all batch tests in Table 2, along with the associated initial NH_4^+ concentration values. The results are the averages of three replicate experiments \pm one standard deviation.

Author Contributions: Conceptualization, M.W. and H.R.; Methodology, M.W. and H.R.; Software, M.W. and H.R.; Validation, M.W. and H.R.; Formal Analysis, M.W. and H.R.; Investigation, M.W. and H.R.; Resources, M.W.; Data Curation, M.W. and H.R.; Writing—Original Draft Preparation, M.W. and H.R.; Writing—Review & Editing, M.W. and H.R.; Visualization, M.W. and H.R.; Supervision, M.W.; Project Administration, M.W.; Funding Acquisition, M.W. All authors have read and agreed to the published version of the manuscript.

Funding: This research received no external funding.

Institutional Review Board Statement: Not applicable.

Informed Consent Statement: Not applicable.

Data Availability Statement: The data presented in this study are available in article and supplementary material.

Conflicts of Interest: The authors declare no conflict of interest.

References

1. Kaza, S.; Yao, L.; Bhada-Tata, P.; Van Woerden, F. *What a Waste 2.0: A Global Snapshot of Solid Waste Management to 2050*; World Bank Publications: Washington, DC, USA, 2018.
2. Kjeldsen, P.; Barlaz, M.A.; Rooker, A.P.; Baun, A.; Ledin, A.; Christensen, T.H. Present and long-term composition of MSW landfill leachate: A review. *Crit. Rev. Environ. Sci. Technol.* **2002**, *32*, 297–336. [[CrossRef](#)]
3. Shin, K.W.; Kim, S.-H.; Kim, J.-H.; Hwang, S.D.; Kang, J.-C. Toxic effects of ammonia exposure on growth performance, hematological parameters, and plasma components in rockfish, *Sebastes schlegelii*, during thermal stress. *Fish. Aquat. Sci.* **2016**, *19*, 1–8. [[CrossRef](#)] [[PubMed](#)]

4. Chamem, O.; Fellner, J.; Zairi, M. Ammonia inhibition of waste degradation in landfills—A possible consequence of leachate recirculation in arid climates. *Waste Manag. Res.* **2020**, *38*, 1078–1086. [[CrossRef](#)] [[PubMed](#)]
5. Liu, Y.; Ngo, H.H.; Guo, W.; Peng, L.; Wang, D.; Ni, B. The roles of free ammonia (FA) in biological wastewater treatment processes: A review. *Environ. Int.* **2019**, *123*, 10–19. [[CrossRef](#)] [[PubMed](#)]
6. Chen, Y.; Cheng, J.J.; Creamer, K.S. Inhibition of anaerobic digestion process: A review. *Bioresour. Technol.* **2008**, *99*, 4044–4064. [[CrossRef](#)]
7. Hafner, S.D.; Bisogni, J.J.; Jewell, W.J. Measurement of un-ionized ammonia in complex mixtures. *Environ. Sci. Technol.* **2006**, *40*, 1597–1602. [[CrossRef](#)]
8. Liu, T.; Sung, S. Ammonia inhibition on thermophilic aceticlastic methanogens. *Water Sci. Technol.* **2002**, *45*, 113–120. [[CrossRef](#)]
9. Procházka, J.; Dolejš, P.; Máca, J.; Dohányos, M. Stability and inhibition of anaerobic processes caused by insufficiency or excess of ammonia nitrogen. *Appl. Microbiol. Biotechnol.* **2012**, *93*, 439–447. [[CrossRef](#)]
10. Strik, D.; Domnanovich, A.; Holubar, P. A pH-based control of ammonia in biogas during anaerobic digestion of artificial pig manure and maize silage. *Process Biochem.* **2006**, *41*, 1235–1238. [[CrossRef](#)]
11. Sung, S.; Liu, T. Ammonia inhibition on thermophilic anaerobic digestion. *Chemosphere* **2003**, *53*, 43–52. [[CrossRef](#)]
12. Cheung, K.C.; Chu, L.M.; Wong, M.H. Ammonia stripping as a pretreatment for landfill leachate. *Water Air Soil Pollut.* **1997**, *94*, 209–221. [[CrossRef](#)]
13. Jurczyk, Ł.; Koc-Jurczyk, J.; Masłoń, A. Simultaneous stripping of ammonia from leachate: Experimental insights and key microbial players. *Water* **2020**, *12*, 2494. [[CrossRef](#)]
14. Kim, D.; Ryu, H.-D.; Kim, M.-S.; Kim, J.; Lee, S.-I. Enhancing struvite precipitation potential for ammonia nitrogen removal in municipal landfill leachate. *J. Hazard. Mater.* **2007**, *146*, 81–85. [[CrossRef](#)] [[PubMed](#)]
15. Warmadewanthi, I.; Zulkarnain, M.A.; Ikhlas, N.; Kurniawan, S.B.; Abdullah, S.R.S. Struvite precipitation as pretreatment method of mature landfill leachate. *Bioresour. Technol. Rep.* **2021**, *15*, 100792. [[CrossRef](#)]
16. Siciliano, A.; Limonti, C.; Curcio, G.M.; Molinari, R. Advances in struvite precipitation technologies for nutrients removal and recovery from aqueous waste and wastewater. *Sustainability* **2020**, *12*, 7538. [[CrossRef](#)]
17. Rahman, M.M.; Salleh, M.A.M.; Rashid, U.; Ahsan, A.; Hossain, M.M.; Ra, C.S. Production of slow release crystal fertilizer from wastewaters through struvite crystallization—A review. *Arab. J. Chem.* **2014**, *7*, 139–155. [[CrossRef](#)]
18. Li, X.; Zhao, Q.; Hao, X. Ammonium removal from landfill leachate by chemical precipitation. *Waste Manag.* **1999**, *19*, 409–415. [[CrossRef](#)]
19. Siciliano, A. Assessment of fertilizer potential of the struvite produced from the treatment of methanogenic landfill leachate using low-cost reagents. *Environ. Sci. Pollut. Res.* **2016**, *23*, 5949–5959. [[CrossRef](#)]
20. Darwish, M.; Aris, A.; Puteh, M.H.; Jusoh, M.; Kadir, A.A. Waste bones ash as an alternative source of P for struvite precipitation. *J. Environ. Manag.* **2017**, *203*, 861–866. [[CrossRef](#)]
21. Huang, H.; Xiao, D.; Zhang, Q.; Ding, L. Removal of ammonia from landfill leachate by struvite precipitation with the use of low-cost phosphate and magnesium sources. *J. Environ. Manag.* **2014**, *145*, 191–198. [[CrossRef](#)]
22. Chen, L.; Zhou, C.H.; Zhang, H.; Tong, D.S.; Yu, W.H.; Yang, H.M.; Chu, M.Q. Capture and recycling of ammonium by dolomite-aided struvite precipitation and thermolysis. *Chemosphere* **2017**, *187*, 302–310. [[CrossRef](#)]
23. Katakai, S.; West, H.; Clarke, M.; Baruah, D.C. Phosphorus recovery as struvite: Recent concerns for use of seed, alternative Mg source, nitrogen conservation and fertilizer potential. *Resour. Conserv. Recycl.* **2016**, *107*, 142–156. [[CrossRef](#)]
24. Enyemadze, I.; Momade, F.W.; Oduro-Kwarteng, S.; Essandoh, H. Phosphorus recovery by struvite precipitation: A review of the impact of calcium on struvite quality. *J. Water Sanit. Hyg. Dev.* **2021**, *11*, 706–718. [[CrossRef](#)]
25. Le Corre, K.S.; Valsami-Jones, E.; Hobbs, P.; Parsons, S.A. Impact of calcium on struvite crystal size, shape and purity. *J. Cryst. Growth* **2005**, *283*, 514–522. [[CrossRef](#)]
26. Liu, X.; Wang, J. Impact of calcium on struvite crystallization in the wastewater and its competition with magnesium. *Chem. Eng. J.* **2019**, *378*, 122121. [[CrossRef](#)]
27. Moragaspiya, C.; Rajapakse, J.; Millar, G.J. Effect of Ca:Mg ratio and high ammoniacal nitrogen on characteristics of struvite precipitated from waste activated sludge digester effluent. *J. Environ. Sci.* **2019**, *86*, 65–77. [[CrossRef](#)]
28. Li, W.; Ding, X.; Liu, M.; Guo, Y.; Liu, L. Optimization of process parameters for mature landfill leachate pretreatment using MAP precipitation. *Front. Environ. Sci. Eng.* **2012**, *6*, 892–900. [[CrossRef](#)]
29. Li, X.; Zhao, Q. MAP precipitation from landfill leachate and seawater bittern waste. *Environ. Technol.* **2002**, *23*, 989–1000. [[CrossRef](#)]
30. Amrulloh, H.; Simanjuntak, W.; Situmeang, R.T.M.; Sagala, S.L.; Bramawanto, R.; Fatiqin, A.; Nahrowi, R.; Zuniati, M. Preparation of nano-magnesium oxide from Indonesia local seawater bittern using the electrochemical method. *Inorg. Nano-Met. Chem.* **2020**, *50*, 693–698. [[CrossRef](#)]
31. Bagastyo, A.Y.; Satria, A.Z.; Anggrainy, A.D.; Affandi, K.A.; Kartika, S.W.T.; Nurhayati, E. Resource recovery and utilization of bittern wastewater from salt production: A review of recovery technologies and their potential applications. *Environ. Technol. Rev.* **2021**, *10*, 295–322. [[CrossRef](#)]
32. Shin, H.-S.; Lee, S. Removal of nutrients in wastewater by using magnesium salts. *Environ. Technol.* **1998**, *19*, 283–290. [[CrossRef](#)]
33. Etter, B.; Tilley, E.; Khadka, R.; Udert, K.M. Low-cost struvite production using source-separated urine in Nepal. *Water Res.* **2011**, *45*, 852–862. [[CrossRef](#)] [[PubMed](#)]

34. Halwani, J.; Halwani, B.; Amine, H.; Kabbara, M.B. Waste management in Lebanon—Tripoli case study. In *Waste Management in MENA Regions*; Springer: Cham, Switzerland, 2020; pp. 223–239.
35. Camargo, C.; Guimarães, J.; Tonetti, A. Treatment of landfill leachate: Removal of ammonia by struvite formation. *Water SA* **2014**, *40*, 491–494. [[CrossRef](#)]
36. Siciliano, A.; Stillitano, M.A.; Limonti, C.; Marchio, F. Ammonium removal from landfill leachate by means of multiple recycling of struvite residues obtained through acid decomposition. *Appl. Sci.* **2016**, *6*, 375. [[CrossRef](#)]
37. Cao, X.; Ma, L.Q.; Chen, M.; Singh, S.P.; Harris, W.G. Impacts of phosphate amendments on lead biogeochemistry at a contaminated site. *Environ. Sci. Technol.* **2002**, *36*, 5296–5304. [[CrossRef](#)] [[PubMed](#)]
38. McGowen, S.; Basta, N.; Brown, G. Use of diammonium phosphate to reduce heavy metal solubility and transport in smelter-contaminated soil. *J. Environ. Qual.* **2001**, *30*, 493–500. [[CrossRef](#)]
39. Sposito, G. *The Chemistry of Soils*; Oxford Univ. Press: New York, NY, USA, 1989.
40. Gustafsson, J.P. *Visual MINTEQ 3.0 User Guide*; KTH, Department of Land and Water Resources: Stockholm, Sweden, 2011.
41. Langmuir, D. *Aqueous Environmental Geochemistry*; Prentice Hall: Hoboken, NJ, USA, 1997.
42. Luo, H.; Zeng, Y.; Cheng, Y.; He, D.; Pan, X. Recent advances in municipal landfill leachate: A review focusing on its characteristics, treatment, and toxicity assessment. *Sci. Total Environ.* **2020**, *703*, 135468. [[CrossRef](#)]
43. Teng, C.; Zhou, K.; Peng, C.; Chen, W. Characterization and treatment of landfill leachate: A review. *Water Res.* **2021**, *203*, 117525. [[CrossRef](#)]
44. Anthonisen, A.C.; Loehr, R.C.; Prakasam, T.; Srinath, E. Inhibition of nitrification by ammonia and nitrous acid. *J. Water Pollut. Control Fed.* **1976**, *48*, 835–852.
45. Çelen, I.; Türker, M. Recovery of ammonia as struvite from anaerobic digester effluents. *Environ. Technol.* **2001**, *22*, 1263–1272. [[CrossRef](#)]
46. El Diwani, G.; El Rafie, S.; El Ibiari, N.; El-Aila, H. Recovery of ammonia nitrogen from industrial wastewater treatment as struvite slow releasing fertilizer. *Desalination* **2007**, *214*, 200–214. [[CrossRef](#)]
47. Lee, S.; Weon, S.; Lee, C.; Koopman, B. Removal of nitrogen and phosphate from wastewater by addition of bittern. *Chemosphere* **2003**, *51*, 265–271. [[CrossRef](#)]
48. Siciliano, A.; Rosa, S.D. Recovery of ammonia in digestates of calf manure through a struvite precipitation process using unconventional reagents. *Environ. Technol.* **2014**, *35*, 841–850. [[CrossRef](#)] [[PubMed](#)]
49. Huang, H.; Chen, Y.; Jiang, Y.; Ding, L. Treatment of swine wastewater combined with MgO-saponification wastewater by struvite precipitation technology. *Chem. Eng. J.* **2014**, *254*, 418–425. [[CrossRef](#)]
50. Tonetti, A.L.; de Camargo, C.C.; Guimarães, J.R. Ammonia removal from landfill leachate by struvite formation: An alarming concentration of phosphorus in the treated effluent. *Water Sci. Technol.* **2016**, *74*, 2970–2977. [[CrossRef](#)] [[PubMed](#)]
51. Doyle, J.D.; Parsons, S.A. Struvite formation, control and recovery. *Water Res.* **2002**, *36*, 3925–3940. [[CrossRef](#)]
52. Maekawa, T.; Liao, C.-M.; Feng, X.-D. Nitrogen and phosphorus removal for swine wastewater using intermittent aeration batch reactor followed by ammonium crystallization process. *Water Res.* **1995**, *29*, 2643–2650. [[CrossRef](#)]
53. Korchef, A.; Saidou, H.; Amor, M.B. Phosphate recovery through struvite precipitation by CO₂ removal: Effect of magnesium, phosphate and ammonium concentrations. *J. Hazard. Mater.* **2011**, *186*, 602–613. [[CrossRef](#)]
54. Kumar, R.; Pal, P. Turning hazardous waste into value-added products: Production and characterization of struvite from ammoniacal waste with new approaches. *J. Clean. Prod.* **2013**, *43*, 59–70. [[CrossRef](#)]
55. Caceres, P.; Attiogbe, E. Thermal decomposition of dolomite and the extraction of its constituents. *Miner. Eng.* **1997**, *10*, 1165–1176. [[CrossRef](#)]
56. Valverde, J.M.; Perejon, A.; Medina, S.; Perez-Maqueda, L.A. Thermal decomposition of dolomite under CO₂: Insights from TGA and in situ XRD analysis. *Phys. Chem. Chem. Phys.* **2015**, *17*, 30162–30176. [[CrossRef](#)]
57. Kiani, D.; Silva, M.; Sheng, Y.; Baltrusaitis, J. Experimental insights into the genesis and growth of struvite particles on low-solubility dolomite mineral surfaces. *J. Phys. Chem. C* **2019**, *123*, 25135–25145. [[CrossRef](#)]
58. Li, B.; Boiarkina, I.; Young, B.; Yu, W. Quantification and mitigation of the negative impact of calcium on struvite purity. *Adv. Powder Technol.* **2016**, *27*, 2354–2362. [[CrossRef](#)]
59. Romero-Güiza, M.; Astals, S.; Mata-Alvarez, J.; Chimenos, J.M. Feasibility of coupling anaerobic digestion and struvite precipitation in the same reactor: Evaluation of different magnesium sources. *Chem. Eng. J.* **2015**, *270*, 542–548. [[CrossRef](#)]